Chemical Science

EDGE ARTICLE

View Article Online
View Journal | View Issue

Cite this: *Chem. Sci.*, 2019, **10**, 1873

All publication charges for this article have been paid for by the Royal Society of Chemistry

Fluorogenic hydrogen sulfide (H_2S) donors based on sulfenyl thiocarbonates enable H_2S tracking and quantification†

Yu Zhao, Matthew M. Cerda and Michael D. Pluth *

Received 21st November 2018
Accepted 10th December 2018

DOI: 10.1039/c8sc05200j

rsc.li/chemical-science

Hydrogen sulfide (H_2S) is an important cellular signaling molecule that exhibits promising protective effects. Although a number of triggerable H_2S donors have been developed, spatiotemporal feedback from H_2S release in biological systems remains a key challenge in H_2S donor development. Herein we report the synthesis, evaluation, and application of caged sulfenyl thiocarbonates as new fluorescent H_2S donors. These molecules rely on thiol cleavage of sulfenyl thiocarbonates to release carbonyl sulfide (COS), which is quickly converted to H_2S by carbonic anhydrase (CA). This approach is a new strategy in H_2S release and does not release electrophilic byproducts common from COS-based H_2S releasing motifs. Importantly, the release of COS/H_2S is accompanied by the release of a fluorescent reporter, which enables the real-time tracking of H_2S by fluorescence spectroscopy or microscopy. Dependent on the choice of fluorophore, either one or two equivalents of H_2S can be released, thus allowing for the dynamic range of the fluorescent donors to be tuned. We demonstrate that the fluorescence response correlates directly with quantified H_2S release and also demonstrate the live-cell compatibility of these donors. Furthermore, these fluorescent donors exhibit anti-inflammatory effects in RAW 264.7 cells, indicating their potential application as new H_2S-releasing therapeutics. Taken together, sulfenyl thiocarbonates provide a new platform for H_2S donation and readily enable fluorescent tracking of H_2S delivery in complex environments.

Introduction

Hydrogen sulfide (H_2S) is an important gaseous molecule that plays critical roles in living systems.[1–3] Endogenous H_2S is primarily produced from cysteine (Cys) and homocysteine (Hcy) by four main enzymes, including cystathionine β-synthase (CBS), cystathionine γ-lyase (CSE), 3-mercaptopyruvate sulfur transferase (3-MST), and cysteine aminotransferase (CAT).[4–8] Due to its bioregulatory and protective roles, H_2S is considered as an important cellular signaling molecule, much like nitric oxide (NO) and carbon monoxide (CO).[8–11]

Although many H_2S-related biological functions have been discovered in the past two decades, many investigations have been limited due to the lack of controllable and refined H_2S delivery systems (H_2S donors). Inorganic sulfide salts, such as sodium sulfide (Na_2S) and sodium hydrosulfide (NaHS), are widely used in H_2S investigations, but they release H_2S quickly in aqueous media, thus failing to mimic the slow and well-regulated *in vivo* H_2S generation.[12] By contrast, the H_2S release from GYY4137, a phosphorodithioate-based H_2S donor, is slow in aqueous buffer, and the low H_2S releasing efficiency remains as a major concern when applying it to the living systems.[13] Building from these donor scaffolds, a series of synthetic H_2S donors have been developed in the last decade.[14–19] These donors are activated by different triggers, such as enzymes,[20,21] cellular thiols,[22–27] pH modulation,[28,29] and photo activation,[30–33] and the released H_2S exhibits promising activities in different physiological and pathological processes.[17,18]

To expand the library of H_2S donors, we recently developed the carbonyl sulfide (COS)-based platform for H_2S donation. In this approach, caged-thiocarbamates are activated and the resultant intermediates undergo a cascade reaction to release COS, which is quickly converted to H_2S by the ubiquitous enzyme carbonic anhydrase (CA) (Fig. 1a).[34] Expanding on this initial report, we, as well as others, have applied the similar caged-COS systems to include a series of triggerable COS-based H_2S donors which can be activated by different mechanisms, such as reactive oxygen species (ROS),[35–37] esterase,[38,39] cellular nucleophiles,[40] click chemistry,[41] light,[42–44] and Cys,[45] to release H_2S under various conditions.[45,46]

Although H_2S release from these donors has been measured using different methods, the real-time tracking of donor activation and H_2S delivery in living systems remains a key challenge due to the inherent limitations of current H_2S detection

Department of Chemistry and Biochemistry, Institute of Molecular Biology, Materials Science Institute, University of Oregon, Eugene, OR 97403, USA. E-mail: pluth@uoregon.edu

† Electronic supplementary information (ESI) available: H_2S release curves, cytotoxicity data, NMR spectra. See DOI: 10.1039/c8sc05200j

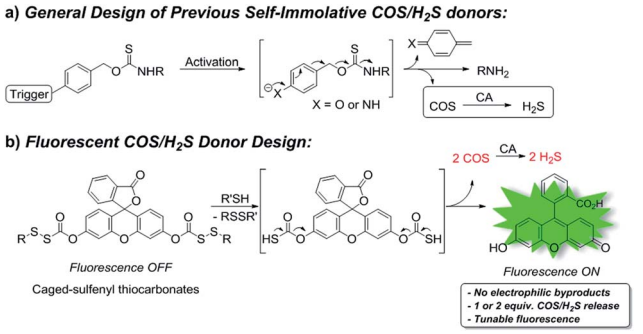

Fig. 1 (a) General design of previous self-immolative COS/H_2S donors. (b) COS/H_2S release from fluorogenic caged-sulfenyl thiocarbonate donor motifs.

methods. For example, the colorimetric methylene blue (MB) assay has been widely used to measure H_2S levels, but requires strongly acidic conditions, which may trigger H_2S release from acid labile sulfide pools. Additionally, MB is an end-point assay which destroys experimental samples, thus making it not feasible for *in vivo* H_2S detection.[47] Similarly, H_2S-selective electrodes are most often used in bulk measurements rather than non-homogenized biological samples.[47] By contrast, H_2S fluorescent probes have attracted much attentions due to their high sensitivities and have been used to sense and visualize H_2S in biological samples.[48] Albeit promising, H_2S fluorescent probes are prone to react with reactive cellular species, such as Cys or glutathione (GSH), which results in either probe consumption or false positive signals. In addition, all of the above methods consume the H_2S being measured. Recently, we reported a series of γ-ketothiocarbamates (γ-KetoTCM) that release *p*-nitroaniline as a colorimetric indicator; however, although the colorimetric response enables monitoring of COS/H_2S release in cuvettes, the direct tracking in live-cell environments remains an un-met need.[49] Taken together, a key advancement compatible with live-cell and tissue experiments would be the development of H_2S donors that deliver H_2S with a concomitant fluorescence response to enable tracking of H_2S delivery by common microscopy techniques.

Aligned with these needs, we report here the development of a new H_2S-releasing strategy based on caged sulfenyl thiocarbonates and apply this donor platform to access fluorescent turn-on H_2S donors. In this approach, cellular thiols (*i.e.* Cys and GSH) activate the sulfenyl thiocarbonates through thiol-mediated disulfide reduction to release COS, which is quickly converted to H_2S by CA (Fig. 1b). To the best of our knowledge, the sulfenyl thiocarbonate reduction strategy provides a new activation pathway that has not been used to trigger COS/H_2S release from donor platforms. Unlike currently-available donors that function through initial COS release, the sulfenyl thiocarbonate system does not generate reactive electrophile byproducts upon activation, which provides a significant advance in the field. In addition, we leverage this new donor strategy to access systems in which a concomitant fluorescence turn-on occurs upon donor activation, thus allowing for real-time monitoring and quantification of H_2S release using fluorescence spectroscopy.

Results and discussion

To test our hypothesis that caged-sulfenyl thiocarbonates could serve as thiol-triggered fluorescent COS/H_2S donors, four donors (**FLD-1–4**) were prepared by reacting fluorescein or 3-*O*-methylfluorescein with ((benzyl)dithio)carbonyl chloride **1** or ((phenol)dithio)carbonyl chloride **2** in the presence of DIPEA (Scheme 1a). A caged thiocarbonate (**TCN-1**) was synthesized as a triggerless control compound, which is expected to be stable toward thiol activation due to the lack of a disulfide functional group (Scheme 1b).

With these compounds in hand, we first evaluated their spectroscopic properties in PBS buffer (pH 7.4, 10 mM). As expected, **FLD-1–3** and **TCN-1** are not absorptive in the visible region and are all nonfluorescent because the fluorescein unit is locked in the closed lactone form. By contrast, **FLD-4** shows a prominent absorbance band in the visible region (λ_{max} = 449 nm, ε = 27 300 ± 2500 M^{-1} cm^{-1}) with measurable fluorescence (λ_{em} = 514 nm, Φ = 0.11 ± 0.01) due to the free hydroxyl group (Table S1†). Based on the promising spectroscopic properties, large dynamic range, and efficient release of two equivalents of COS/H_2S, we chose to use **FLD-1** as the model donor for initial reactivity and selectivity evaluations.

To test the reactivity of **FLD-1** towards Cys-induced activation, **FLD-1** (10 μM) was incubated with Cys (100 μM) in PBS buffer (pH 7.4, 10 mM) containing physiologically-relevant concentrations of CA (25 μg mL^{-1}), and the fluorescence intensity was measured using a fluorescence spectrometer. As expected, Cys successfully activated **FLD-1** and resulted in a 500-fold fluorescence turn on over 2 h, demonstrating the release of the fluorescein upon **FLD-1** activation (Fig. 2a). Fluorescein formation was also confirmed by UV-vis spectroscopy under the identical conditions (Fig. S1†). A Cys-dependent fluorescence enhancement was observed when treating **FLD-1** (10 μM) with increasing concentrations of Cys (1–20 equiv.), indicating a high sensitivity of **FLD-1** towards Cys. No fluorescent signal was observed in the absence of Cys, suggesting that **FLD-1** is stable in aqueous buffer, and that it is not hydrolyzed to provide false

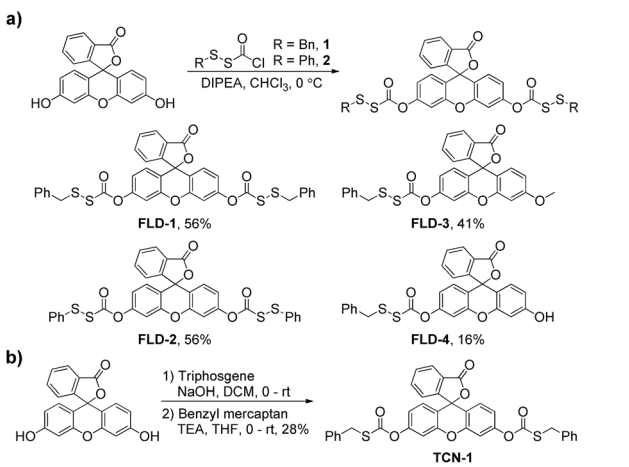

Scheme 1 Synthesis of fluorescent COS/H_2S donors (a) and thiocarbonate control compound (b).

signals (Fig. 2b). In addition, to confirm the H_2S delivery from **FLD-1**, we treated **FLD-1** (10 μM) with Cys (100 μM) in PBS containing CA (25 μg mL^{-1}) and quantified H_2S release using the MB assay. In this experiment, 15 μM of H_2S was detected (75% releasing efficiency), which is consistent with our hypothesis that 2 equivalents of COS/H_2S would be released upon **FLD-1** activation (Fig. S2†). Taken together, these experiments demonstrate that **FLD-1** is highly responsive to Cys activation.

To determine whether H_2S release correlated directly with the observed fluorescence response, we measured the fluorescent response from **FLD-3** in the presence of Cys and CA and quantified H_2S release using the MB assay. We chose to use **FLD-3** as the model compound for these investigations because it only contains one sulfenyl thiocarbonate moiety, and therefore should simplify the reaction kinetics. In comparison, **FLD-1** contains two sulfenyl thiocarbonate groups, and the cleavage of one sulfenyl thiocarbamate would generate **FLD-4** as a reaction intermediate, which exhibits moderate fluorescence (see Fig. 4). Incubation of **FLD-3** (10 μM) with Cys (100 μM) resulted in a rapid fluorescence response with 96% of the H_2S release measured by MB. At extended time points, we observed a slight decrease in measured H_2S, possibly due to volatilization of H_2S in the headspace of the closed system or adventitious oxidation of released H_2S. Negligible H_2S was detected in the absence of CA, indicating that Cys-triggered H_2S delivery from **FLD-3** proceeds through intermediate COS formation (Fig. 3a). Importantly, the strong linear correlation between the measured fluorescence and H_2S measured from the MB method detection (first 25 min, $R^2 = 0.988$) demonstrates that fluorescent readouts can serve as reliable optical tools to track COS/H_2S release from **FLD** donors with temporal resolution (Fig. 3b). Moreover, this linear correlation suggests that choice of other fluorophores with different brightnesses and photophysical properties could be used to access different dynamic ranges of H_2S release, thus enabling this approach to be translated to different types of experimental designs.

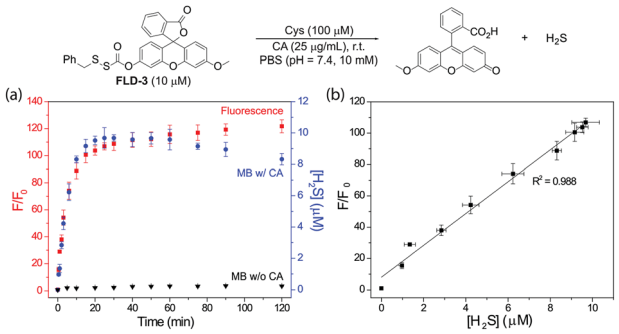

Fig. 3 (a) Time-dependent fluorescence turn on (red) and H_2S release (blue) upon **FLD-3** (10 μM) activation in PBS (pH 7.4, 10 mM) containing Cys (100 μM) and CA (25 μg mL^{-1}). No H_2S was detected in the absence of CA (black). $\lambda_{ex} = 454$ nm, $\lambda_{em} = 500–650$ nm, and slit width = 0.3 mm. (b) Correlation between fluorescence measurement and MB detection. The experiments were performed in triplicate. The results are expressed as mean ± SD ($n = 3$).

Having confirmed the efficiency of Cys-triggered fluorescence turn on and COS/H_2S release, we next evaluated the reactivity of other **FLD** donors towards Cys activation. Treating **FLD-1–3** (10 μM) with Cys (100 μM) in PBS buffer (pH 7.4, 10 mM) resulted in a 120–500-fold fluorescence turn on over 2 h. We attribute the faster response of **FLD-2** to the more electrophilic phenyl sulfenyl thiocarbonate in comparison to the less electrophilic benzyl sulfenyl thiocarbonate in **FLD-1**. **FLD-4**, however, provided minimal fluorescence enhancement due to its strong background fluorescence. No fluorescence response from **TCN-1** (10 μM) was observed under the identical conditions, which demonstrates the stability of the thiocarbonate group in the presence of Cys (Fig. 4).

To further support our proposed activation mechanism in Fig. 1b, as well as the activation of the sulfenyl thiocarbonate group by other thiols, we incubated **FLD-1** (10 μM) in PBS

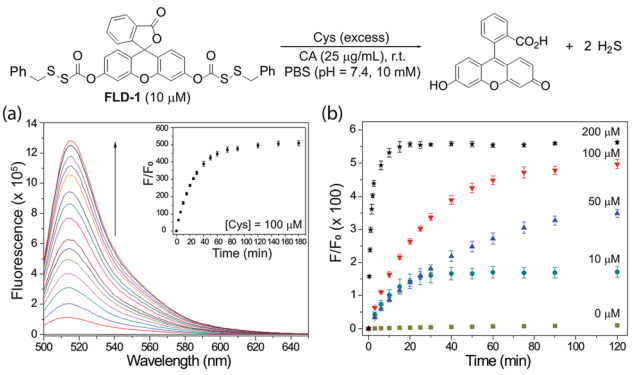

Fig. 2 (a) Time-dependent fluorescence spectra of **FLD-1** (10 μM) in PBS (pH 7.4, 10 mM) containing Cys (100 μM) and CA (25 μg mL^{-1}). (b) Cys-dependent (0–200 μM) fluorescence turn on of **FLD-1** (10 μM) in PBS. $\lambda_{ex} = 490$ nm, $\lambda_{em} = 500–650$ nm, and slit width = 0.3 mm. The experiments were performed in triplicate and results are expressed as mean ± SD ($n = 3$).

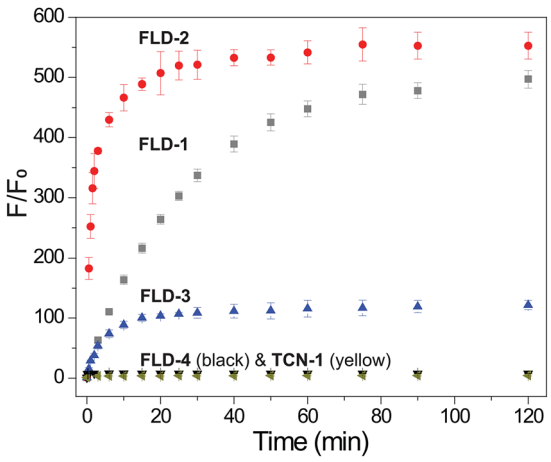

Fig. 4 Fluorescence turn on of **FLD-1** (gray), **FLD-2** (red), **FLD-3** (blue), **FLD-4** (black), and **TCN-1** (dark yellow) (10 μM) in PBS (pH 7.4, 10 mM) containing Cys (100 μM). $\lambda_{ex} = 490$ nm for **FLD-1**, **2**, **4**, and **TCN-1**, $\lambda_{ex} = 454$ nm for **FLD-3**, $\lambda_{em} = 500–650$ nm, and slit width = 0.3 mm. The experiments were performed in triplicate. The results are expressed as mean ± SD ($n = 3$).

(pH 7.4, 10 mM) with 10 equivalents of benzyl mercaptan (100 μM) for 1 h and analyzed the reaction products by HPLC (Fig. S3†). Consistent with our proposed activation mechanism, we observed **FLD-1** consumption and the formation of both benzyl disulfide and fluorescein, which supports the proposed mechanism.

In addition to Cys and BnSH, other cellular thiols and biological nucleophiles were tested to determine whether they resulted in donor activation. In these experiments, **FLD-1** (10 μM) was incubated with GSH, homocysteine (Hcy), *N*-acetyl cysteine (NAC), penicillamine (PEN), or bovine serum albumin (BSA) (100 μM), in PBS buffer (pH 7.4, 10 mM) containing CA (25 μg mL^{-1}) and the fluorescent intensity was measured after 2 h. As expected, **FLD-1** is stable in PBS at physiological pH in the absence of thiols (Fig. 5 bar 1). Incubation of **FLD-1** with Cys, NAC, GSH, and Hcy, however, led to a significant fluorescence enhancement, indicating successful donor activation and COS/H_2S release (Fig. 5 bars 2–5 and S4†). In addition, these results demonstrate that the sulfenyl thiocarbonate group is responsive to different types of thiols. In comparison, PEN resulted in only minimal fluorescence response and BSA failed to activate the donor presumably due to the bulkiness of these two thiol species, which hindered their reactions with **FLD-1** (Fig. 5 bars 6 and 7). Additionally, *N*-ethylmaleimide (NEM) pretreatment of Cys samples significantly reduced the fluorescence enhancement from **FLD-1**, confirming the necessity of the thiol-induced reduction for the donor activation (Fig. 5 bar 8).

We also tested the response of the **FLD** donors in the presence of other cellular reactive sulfur, oxygen, and nitrogen species (RSONs). **FLD-1** (10 μM) was incubated with RSONs (100 μM), such as hydrogen peroxide (H_2O_2), hyperchlorite (ClO^-), superoxide (O_2^-), *tert*-butyl hydroperoxide (TBHP), serine (Ser), lysine (Lys), glycine (Gly), oxidized glutathione (GSSG), and *S*-nitrosoglutathione (GSNO), and COS/H_2S release was monitored by tracking the fluorescein formation. As expected, minimal fluorescence was observed in these experiments, confirming the stability of **FLD-1** to common RSONs (Fig. 5 bars 9–17). Because the carbonate functional group may be sensitive to esterase-catalyzed hydrolysis, we also tested the esterase stability of the sulfenyl thiocarbonate group by incubating **FLD-1** (10 μM) with porcine liver esterase (PLE, 1 U mL^{-1}). Although a slight fluorescence turn on was observed after a 2 h incubation, the observed response was much lower than that from thiol activation (Fig. 5 bar 18). Taken together, these studies demonstrate that **FLD-1** is highly responsive and selective to thiol activation and common cellular RSONs do not trigger **FLD-1** to release COS/H_2S.

After confirming the thiol-triggered COS/H_2S release from **FLD-1** in aqueous buffer, we next investigated the H_2S delivering capacity of **FLD-1** in cellular environment. In these experiments, HeLa cells were treated with **FLD-1** (50 μM) or **TCN-1** (50 μM) and H_2S release was monitored using C7-Az, a H_2S-responsive fluorescent probe.[50,51] Incubation of HeLa cells with C7-Az (50 μM) alone resulted in a negligible fluorescence response, indicating minimal endogenous H_2S (Fig. 6 top row). Treatment with **TCN-1** also failed to provide a fluorescence signal, suggesting that the thiocarbonate group was stable and did not decompose to generate false signals in cellular environments (Fig. 6 middle row). By contrast, a strong C7-Az fluorescent signal was observed when incubating HeLa cells with **FLD-1**, suggesting that H_2S release was successfully triggered by endogenous thiols. In addition, a strong fluorescence signal was also observed from activated **FLD-1** in the fluorescein channel, confirming the fluorescence response upon donor activation (Fig. 6 bottom row). Taken together, these results demonstrate that the **FLD** donors not only function as efficacious H_2S donors in live cells, but also provide a fluorescence signal that enables observing H_2S release.

To further demonstrate the H_2S-releasing fidelity of the **FLD** donors we also investigated the anti-inflammatory activities of **FLD-1**. We pretreated macrophage RAW 264.7 cells with **FLD-1** (0–25 μM) for 2 h, followed by a 24 h incubation with lipopolysaccharide (LPS, 0.5 μg mL^{-1}) to trigger the inflammatory

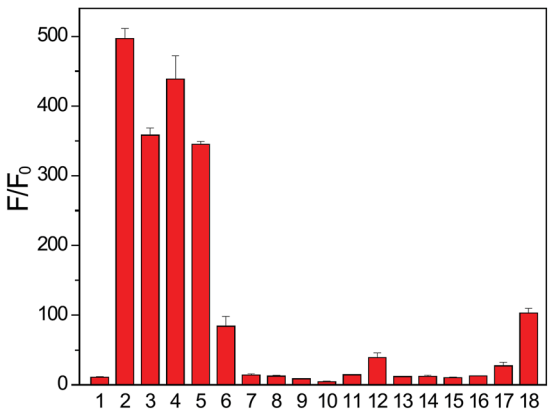

Fig. 5 Fluorescence turn on of **FLD-1** (10 μM) in the presence of cellular RSONs (100 μM): (1) **FLD-1** only, (2) Cys, (3) NAC, (4) GSH, (5) Hcy, (6) PEN, (7) BSA, (8) Cys + NEM, (9) H_2O_2, (10) ClO^-, (11) O_2^-, (12) TBHP, (13) Ser, (14) Lys, (15) Gly, (16) GSSG, (17) GSNO, and (18) PLE (1 U mL^{-1}). Fluorescence intensity was measured after 2 h incubation. The experiments were performed in triplicate. The results were expressed as mean ± SD ($n = 3$).

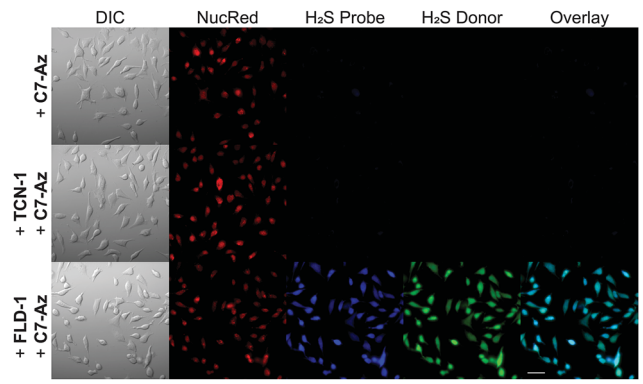

Fig. 6 H_2S delivery from **FLD-1** in HeLa cells. HeLa cells were treated with NucRed nuclear dye and C7-Az (50 μM) in DMEM only (top row) or DMEM containing **TCN-1** (50 μM) (middle row) or **FLD-1** (50 μM) (bottom row) for 30 min. Cells were then washed with PBS and cell images were taken in PBS using a fluorescent microscope. Bar scale: 50 μm.

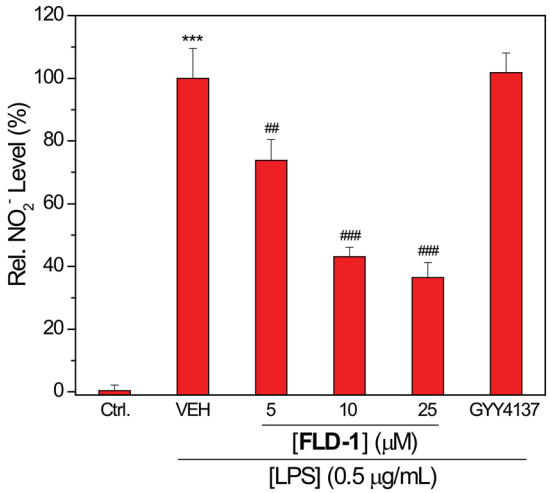

Fig. 7 Effects of **FLD-1** on LPS-induced NO_2^- accumulation. RAW 264.7 cells were pretreated with **FLD-1** (5–25 μM) or GYY4137 (25 μM) for 2 h, followed by a 24 h treatment of LPS (0.5 μg mL^{-1}). Results are expressed as mean ± SD ($n = 4$). ***$P < 0.001$ *vs.* the control group; ##$P < 0.01$ *vs.* vehicle-treated group; ###$P < 0.001$ *vs.* vehicle-treated group.

response. The inflammation event usually results in the NO generation, which can be monitored by measuring nitrite (NO_2^-) accumulation. We chose to use concentrations of **FLD-1** up to 25 μM because these concentrations did not induce cytotoxicity (Fig. S6†).

As expected, the pretreatment of RAW 264.7 cells with **FLD-1** showed a dose-dependent inhibition of NO_2^- accumulation, indicating anti-inflammatory activity from **FLD-1**. Although GYY4137 has shown anti-inflammatory effects at higher concentration and longer incubation time (*i.e.* 100–1000 μM and 24 h incubation),[52] such cytoprotection was not observed at the 25 μM concentration used for comparison, highlighting the efficacious H_2S release from **FLD-1** in the cellular environment (Fig. 7). To further confirm that the observed effects were due to H_2S rather than other components of donor activation, we treated cells with 25 μM of **TCN-1**, fluorescein or benzyl mercaptan and measured NO_2^- production. None of these compounds attenuated NO_2^- generation, confirming that the anti-inflammatory activities of **FLD-1** is due to H_2S release (Fig. S7†). Overall, these studies demonstrate that **FLD-1** releases COS/H_2S in complex cellular environment and exhibits promising anti-inflammatory protections, indicating potential applications of **FLD-1** as H_2S-releasing therapeutics.

Conclusions

In conclusion, we prepared and evaluated a class of caged sulfenyl thiocarbonates as new controllable and fluorescent COS/H_2S donors. Thiol-triggered COS/H_2S release from these molecules has been detected and visualized in both aqueous buffer and in live cells. Importantly, the concomitant release of a fluorescein reporter after H_2S release enables the real-time monitoring of H_2S release dynamics. In addition, we demonstrate that **FLD-1** exhibits a dose-dependent inhibition of the LPS-induced NO formation, which is consistent with anti-inflammatory activities of H_2S. Taken together, caged-sulfenyl thiocarbonates are promising new class of COS/H_2S donors with high potential for accessing H_2S-related protective activities, and the developed fluorescent donors provide new methods for monitoring H_2S release in real-time in complex environments.

Conflicts of interest

There are no conflicts to declare.

Acknowledgements

Research reported in this publication was supported by the NIH (R01GM113030) and Dreyfus Foundation. NMR, fluorescence microscopy, and MS instrumentation in the UO CAMCOR facility is supported by the NSF (CHE-1427987, CHE-1531189, and CHE-1625529).

Notes and references

1 C. Szabo, *Nat. Rev. Drug Discovery*, 2007, **6**, 917–935.
2 R. Wang, *Physiol. Rev.*, 2012, **92**, 791–896.
3 M. R. Filipovic, J. Zivanovic, B. Alvarez and R. Banerjee, *Chem. Rev.*, 2018, **118**, 1253–1337.
4 O. Kabil and R. Banerjee, *Antioxid. Redox Signaling*, 2014, **20**, 770–782.
5 S. Bruce King, *Free Radical Biol. Med.*, 2013, **55**, 1–7.
6 L. F. Hu, M. Lu, P. T. Hon Wong and J. S. Bian, *Antioxid. Redox Signaling*, 2011, **15**, 405–419.
7 B. D. Paul and S. H. Snyder, *Nat. Rev. Mol. Cell Biol.*, 2012, **13**, 499–507.
8 J. M. Fukuto, S. J. Carrington, D. J. Tantillo, J. G. Harrison, L. J. Ignarro, B. A. Freeman, A. Chen and D. A. Wink, *Chem. Res. Toxicol.*, 2012, **25**, 769–793.
9 K. R. Olson, *Antioxid. Redox Signaling*, 2012, **17**, 32–44.
10 C. Szabo, *Antioxid. Redox Signaling*, 2012, **17**, 68–80.
11 L. Li, P. Rose and P. K. Moore, *Annu. Rev. Pharmacol. Toxicol.*, 2011, **51**, 169–187.
12 E. R. DeLeon, G. F. Stoy and K. R. Olson, *Anal. Biochem.*, 2012, **421**, 203–207.
13 L. Li, M. Whiteman, Y. Y. Guan, K. L. Neo, Y. Cheng, S. W. Lee, Y. Zhao, R. Baskar, C. H. Tan and P. K. Moore, *Circulation*, 2008, **117**, 2351–2360.
14 M. D. Pluth, T. S. Bailey, M. D. Hammers, M. D. Hartle, H. A. Henthorn and A. K. Steiger, *Synlett*, 2015, **26**, 2633–2643.
15 C. Szabo and A. Papapetropoulos, *Pharmacol. Rev.*, 2017, **69**, 497–564.
16 M. D. Hartle and M. D. Pluth, *Chem. Soc. Rev.*, 2016, **45**, 6108–6117.
17 Y. Zhao, T. D. Biggs and M. Xian, *Chem. Commun.*, 2014, **50**, 11788–11805.
18 Y. Zhao, A. Pacheco and M. Xian, *Handb. Exp. Pharmacol.*, 2015, **230**, 365–388.

19 C. R. Powell, K. M. Dillon and J. B. Matson, *Biochem. Pharmacol.*, 2018, **149**, 110–123.
20 P. Shukla, V. S. Khodade, M. SharathChandra, P. Chauhan, S. Mishra, S. Siddaramappa, B. E. Pradeep, A. Singh and H. Chakrapani, *Chem. Sci.*, 2017, **8**, 4967–4972.
21 Y. Zheng, B. Yu, K. Ji, Z. Pan, V. Chittavong and B. Wang, *Angew. Chem., Int. Ed.*, 2016, **55**, 4514–4518.
22 J. C. Foster, C. R. Powell, S. C. Radzinski and J. B. Matson, *Org. Lett.*, 2014, **16**, 1558–1561.
23 Y. Zhao, S. Bhushan, C. Yang, H. Otsuka, J. D. Stein, A. Pacheco, B. Peng, N. O. Devarie-Baez, H. C. Aguilar, D. J. Lefer and M. Xian, *ACS Chem. Biol.*, 2013, **8**, 1283–1290.
24 Y. Zhao, H. Wang and M. Xian, *J. Am. Chem. Soc.*, 2011, **133**, 15–17.
25 Y. Zhao, C. Yang, C. Organ, Z. Li, S. Bhushan, H. Otsuka, A. Pacheco, J. Kang, H. C. Aguilar, D. J. Lefer and M. Xian, *J. Med. Chem.*, 2015, **58**, 7501–7511.
26 M. M. Cerda, M. D. Hammers, M. S. Earp, L. N. Zakharov and M. D. Pluth, *Org. Lett.*, 2017, **19**, 2314–2317.
27 Y. Zhao, J. Kang, C. M. Park, P. E. Bagdon, B. Peng and M. Xian, *Org. Lett.*, 2014, **16**, 4536–4539.
28 J. Kang, Z. Li, C. L. Organ, C. M. Park, C. T. Yang, A. Pacheco, D. Wang, D. J. Lefer and M. Xian, *J. Am. Chem. Soc.*, 2016, **138**, 6336–6339.
29 J. Wu, Y. Li, C. He, J. Kang, J. Ye, Z. Xiao, J. Zhu, A. Chen, S. Feng, X. Li, J. Xiao, M. Xian and Q. Wang, *ACS Appl. Mater. Interfaces*, 2016, **8**, 27474–27481.
30 N. O. Devarie-Baez, P. E. Bagdon, B. Peng, Y. Zhao, C. M. Park and M. Xian, *Org. Lett.*, 2013, **15**, 2786–2789.
31 N. Fukushima, N. Ieda, K. Sasakura, T. Nagano, K. Hanaoka, T. Suzuki, N. Miyata and H. Nakagawa, *Chem. Commun.*, 2014, **50**, 587–589.
32 Y. Venkatesh, J. Das, A. Chaudhuri, A. Karmakar, T. K. Maiti and N. D. P. Singh, *Chem. Commun.*, 2018, **54**, 3106–3109.
33 Z. Y. Xiao, T. Bonnard, A. Shakouri-Motlagh, R. A. L. Wylie, J. Collins, J. White, D. E. Heath, C. E. Hagemeyer and L. A. Connal, *Chem.–Eur. J.*, 2017, **23**, 11294–11300.
34 A. K. Steiger, S. Pardue, C. G. Kevil and M. D. Pluth, *J. Am. Chem. Soc.*, 2016, **138**, 7256–7259.
35 Y. Zhao and M. D. Pluth, *Angew. Chem., Int. Ed.*, 2016, **55**, 14638–14642.
36 Y. Zhao, H. A. Henthorn and M. D. Pluth, *J. Am. Chem. Soc.*, 2017, **139**, 16365–16376.
37 P. Chauhan, S. Jos and H. Chakrapani, *Org. Lett.*, 2018, **20**, 3766–3770.
38 P. Chauhan, P. Bora, G. Ravikumar, S. Jos and H. Chakrapani, *Org. Lett.*, 2017, **19**, 62–65.
39 A. K. Steiger, M. Marcatti, C. Szabo, B. Szczesny and M. D. Pluth, *ACS Chem. Biol.*, 2017, **12**, 2117–2123.
40 C. R. Powell, J. C. Foster, B. Okyere, M. H. Theus and J. B. Matson, *J. Am. Chem. Soc.*, 2016, **138**, 13477–13480.
41 A. K. Steiger, Y. Yang, M. Royzen and M. D. Pluth, *Chem. Commun.*, 2017, **53**, 1378–1380.
42 Y. Zhao, S. G. Bolton and M. D. Pluth, *Org. Lett.*, 2017, **19**, 2278–2281.
43 A. K. Sharma, M. Nair, P. Chauhan, K. Gupta, D. K. Saini and H. Chakrapani, *Org. Lett.*, 2017, **19**, 4822–4825.
44 P. Štacko, L. Muchová, L. Vítek and P. Klán, *Org. Lett.*, 2018, **20**, 4907–4911.
45 Y. Zhao, A. K. Steiger and M. D. Pluth, *Chem. Commun.*, 2018, **54**, 4951–4954.
46 P. Bora, P. Chauhan, K. A. Pardeshi and H. Chakrapani, *RSC Adv.*, 2018, **8**, 27359–27374.
47 B. Peng and M. Xian, *Asian J. Org. Chem.*, 2014, **3**, 914–924.
48 V. S. Lin, W. Chen, M. Xian and C. J. Chang, *Chem. Soc. Rev.*, 2015, **44**, 4596–4618.
49 Y. Zhao, A. K. Steiger and M. D. Pluth, *Angew. Chem., Int. Ed.*, 2018, **57**, 13101–13105.
50 B. Chen, W. Li, C. Lv, M. Zhao, H. Jin, J. Du, L. Zhang and X. Tang, *Analyst*, 2013, **138**, 946–951.
51 M. K. Thorson, T. Majtan, J. P. Kraus and A. M. Barrios, *Angew. Chem., Int. Ed.*, 2013, **52**, 4641–4644.
52 M. Whiteman, L. Li, P. Rose, C. H. Tan, D. B. Parkinson and P. K. Moore, *Antioxid. Redox Signaling*, 2010, **12**, 1147–1154.